Water-mediated conformer optimization of benzo-18-crown-6-ether/water system

*Ryoji Kusaka, Yoshiya Inokuchi, and Takayuki Ebata**

Department of Chemistry, Graduate School of Science, Hiroshima University, Higashi-Hiroshima 739-8526, Japan

Abstract

The conformation of benzo-18-crown-6-ether (B18C6) and its water encapsulation in a supersonic beam are investigated by laser-induced fluorescence (LIF), UV-UV hole-burning, IR-UV double-resonance (IR-UV DR), and resonance-enhanced multiphoton ionization (REMPI) spectroscopy with the aid of density functional theory (DFT) calculations at the B3LYP/6-31+G* level. At least four B18C6 conformers and nine B18C6-$(H_2O)_n$ (n = 1-4) clusters are identified in the supersonic beam. IR-UV DR spectra in the CH stretching region suggest that the four B18C6 conformers have conformations different from each other. In contrast, most of the nine B18C6-$(H_2O)_n$ clusters have a very similar B18C6 conformation. IR-UV DR spectra in the OH stretching region provide quite clear pictures of the hydration networks formed on B18C6. In all four B18C6-$(H_2O)_1$ isomers, the water molecule is H-bonded to the two O atoms adjacent to the benzene ring in a "bidentate" and a "bifurcated" manner. One of the four B18C6-$(H_2O)_1$ isomers exhibits a large population, and further hydration networks are preferentially grown on this specific isomer.

1. Introduction

Crown ethers are macrocyclic molecules consisting of several oxyethylene (C–C–O) units. By the simultaneous donation of ether O atoms, crown ethers can form stable complexes with metal and organic cations, neutral molecules, and even anions.[1] In addition, crown ether rings are very flexible, and they can adjust their structure to incorporate guest species with different shapes.[1,2] Because of their complex formation ability, crown ethers are used in many applications such as metal cation extraction,[3] fluoroionophore,[4] and phase transfer catalysis.[5] It is well known that 18-crown-6-ether (18C6) forms an exceptionally stable 1:1 complex with K^+ with high symmetry (D_{3d}); the size of K^+ ion is comparable with the cavity size of 18C6.[1,6,7] Crown ethers also show the type of encapsulation in which a guest species is enclosed by two crown ethers[8,9], or two guests are held by one crown ether.[10,11]

Compared with the encapsulation of atomic guests such as alkali metal ions, the encapsulation of polyatomic molecular guests is much more complicated because of the variety of intermolecular interactions. The investigation on the molecular guest encapsulation of crown ethers has been extensively performed in the condensed phase by use of several methods such as x-ray diffraction, IR spectroscopy, and Raman spectroscopy.[12-17] However, in the condensed phase it is sometimes difficult to distinguish between the interaction of crown ethers-guest species and that of crown ethers-solvent molecules. As a result, the encapsulation mechanism is not completely understood at the molecular level. In this sense, the gas phase condition, which is free from solvent effect, is thought to be ideal for shedding light on the interaction between crown ethers and guests. However, the gas phase experiment had not been carried out for crown ethers until very recently because of the difficulty in introducing them into the gas phase. Bühl and Wipff studied the complex of 18C6-H_3O^+ with density functional theory (DFT) calculations.[18] Very recently, we first reported laser spectroscopic study on benzo-18-crown-6-ether (B18C6, Scheme 1), dibenzo-18-crown-6-ether (DB18C6), and their hydrated clusters in supersonic jets.[19,20] The combination of laser spectroscopy and a cooling by the supersonic jet technique enabled us to determine the conformation and

encapsulation structure of each species unambiguously. For DB18C6, we found that a "boat" conformer is the major species, and water molecules form hydration networks on the "boat" conformer.

In this paper, we extend our study to B18C6 and its hydrated clusters. Since B18C6 has only one benzo group, its crown ring is more flexible than that of DB18C6, and its conformation and hydrated structure can be more complicated. In order to obtain the characteristic information about the conformation of B18C6, IR spectra in the CH stretching region are measured. The encapsulation and growth of the hydration network on B18C6 are investigated using IR spectra in the OH stretching region. To examine the preference for the conformation and encapsulation of water molecules, quantum chemical calculations are performed for the B18C6 conformers and their hydrated clusters. The goal of this study is to elucidate the relationship between the conformation and the hydration of B18C6.

2. Experimental and computational

We applied laser-induced fluorescence (LIF), UV-UV hole-burning, resonance-enhanced multiphoton ionization (REMPI), and IR-UV double-resonance (IR-UV DR) spectroscopy to the study of B18C6-$(H_2O)_n$ (n = 0–4) in a supersonic jet. The S_1–S_0 electronic spectra were observed using LIF, REMPI, UV-UV hole-burning spectroscopy, and the IR spectra in the OH and CH stretching region were measured by IR-UV DR spectroscopy. The measurements of the electronic and IR spectra were carried out individually for each species to avoid the spectral congestion and ambiguity due to the overlap of transitions of several species. Details of the experiment are described in Electronic Supplementary Information (ESI) and our previous papers.[21,22] The geometry optimization and vibrational analysis were performed at the B3LYP/6-31+G* level with GAUSSIAN 03 program package.[23] The energies of the optimized structures were corrected by zero-point vibrational energy. The vibrational frequencies were scaled by the factors of 0.9744 and

0.9524 for the OH and CH stretching vibrations, respectively. The S_1–S_0 electronic transition energies were also calculated using time dependent density functional theory (TDDFT) at the same level.

3. Results and discussion

3.1 Electronic spectra of B18C6 and B18C6-$(H_2O)_n$

Fig. 1 shows the LIF spectra of B18C6 in the origin band region; the spectra in Fig. 1(a) and 1(b) were measured without and with adding water vapor, respectively. The addition of water vapor decreases the intensities of bands M1–M4 and increases those of bands A–I. This result suggests that the bands M1–M4 and A–I are due to B18C6 monomers and B18C6-$(H_2O)_n$ clusters, respectively. As described in our previous paper[19] and in ESI, the UV-UV hole-burning experiments confirm that the bands M1–M4 and A–I arise from different species.

The band M1 (35167 cm^{-1}) is located at a much lower frequency than are the bands M2–M4. The positions of the band A and bands B–D are ~100 cm^{-1} higher in frequency than those of the band M1 and bands M2–M4, respectively. In the case of DB18C6,[20] the band position of the DB18C6-$(H_2O)_1$ isomer is 89 cm^{-1} higher in frequency than that of bare DB18C6. On the basis of the relative position between the bands of bare DB18C6 and DB18C6-$(H_2O)_1$, the band A and bands B–D can be assigned to the B18C6-$(H_2O)_1$ isomers formed by the hydration of the conformer M1 and conformers M2–M4, respectively. The bands E–I, which are further blue-shifted with respect to the bands B–D, are assignable to larger hydrated clusters of the conformers M2–M4. As described in our previous papers,[19,20] the blue shift of the origin band in hydrated clusters is due to the H-bonding between water molecule(s) and the O atom(s) adjacent to benzene ring(s). Therefore, it is probable that the water molecule(s) in the B18C6-$(H_2O)_n$ clusters are H-bonded to the O atom(s) next to the benzene ring (O_1 and O_{16} atoms, Scheme 1).

3.2 IR spectra in the OH stretching region

3.2.1 B18C6-$(H_2O)_1$

Fig. 2(a)–(d) shows the IR-UV DR spectra obtained for the bands A–D. The IR-UV DR spectra were measured by monitoring the decrease of the fluorescence intensities induced by IR transition. Thus, the IR bands were observed as depletions in the IR-UV DR spectra. Since each IR spectrum exhibits two bands due to the OH stretching vibrations, species A–D can be assigned to B18C6-$(H_2O)_1$ clusters. The frequencies of the two IR bands (~3570 and ~3640 cm^{-1}) are lower by ~100 cm^{-1} than those of the symmetric (3657 cm^{-1}) and anti-symmetric (3756 cm^{-1}) OH stretching vibrations of H_2O in the gas phase, respectively.[24] The parallel red shift of the OH stretching vibrations indicates that both of the two OH groups in H_2O are H-bonded to the O atoms of B18C6 (bidentate H-bond). Thus, the two IR bands in each spectrum are assignable to the symmetric and anti-symmetric OH stretching vibrations of a bidentate H_2O molecule in the B18C6-$(H_2O)_1$ isomer. The stick spectra in Fig. 2 are the IR spectra calculated for the optimized structures of B18C6-$(H_2O)_1$, which will be explained later.

3.2.2 B18C6-$(H_2O)_2$

Fig. 3(a) shows the IR-UV DR spectrum of the band E. Four strong bands appear at 3559, 3570, 3637, and 3643 cm^{-1}. The positions of the bands are close to those of the species A–D shown in Fig. 2. Therefore, one can assign the four bands to two pairs of bidentate OH stretching vibrations. Two weak bands labeled by asterisks are located at 3684 and 3689 cm^{-1}. Since the frequency of the dangling OH in H-bonded H_2O is higher than 3700 cm^{-1},[25,26] the two bands are not ascribable to the free OH stretching vibrations of H_2O molecules. These two bands are probably due to intermolecular stretching vibrations associated with the symmetric OH stretching.[27] Thus, species E can be assigned to B18C6-$(H_2O)_2$ in which two H_2O molecules are H-bonded in the bidentate manner. The IR-UV DR spectrum of species F shown in Fig. 3(b) exhibits four bands, indicating

that species F is another isomer of B18C6-$(H_2O)_2$. Compared with the IR spectra of the bands A–D (Fig. 2), one can assign the bands at 3513 and 3595 cm^{-1} to the bidentate OH stretching vibrations. The frequencies of the two bands are lower than those of species A–D by ~60 cm^{-1}. The red shift of the two bidentate OH bands implies that the O atom of a bidentate H_2O accepts a second H_2O molecule. Actually, bands at 3393 and 3715 cm^{-1} are assignable to the singly H-bonded and free OH stretching vibrations, respectively, of the second H_2O molecule. Fig. 3(c) displays the IR-UV DR spectrum of the band G, which exhibits four strong bands at 3536, 3586, 3622, and 3658 cm^{-1} and a weak band at 3641 cm^{-1} (labeled by an asterisk). These bands are located in the region of the bidentate OH stretching vibrations. As seen in Figs. 2(a)–(d) and 3(a), the interval between the two bidentate OH vibrations is ~75 cm^{-1}. Based on the interval, two pairs of the bidentate vibrations are found as shown in Fig. 3(c). We cannot give a definitive assignment for the band marked by the asterisk. Possible assignment for this band is a combination band of the OH stretching vibrations. Therefore, we consider that species G has two bidentate H_2O molecules. The spectral feature of species G is similar to that of species E, although the two band pairs of species G are more separated from each other compared with those of species E.

3.2.3 B18C6-$(H_2O)_{3,4}$

The IR-UV DR spectrum of the band H is displayed in Fig. 4(a). Seven bands are identified in the spectrum. Among them, the weak band at 3228 cm^{-1} is ascribable to the overtone of the bending vibration of H_2O.[28] Accordingly, species H can be assigned to a B18C6-$(H_2O)_3$ cluster. The four bands in the 3500–3650 cm^{-1} region are assignable to two pairs of the bidentate OH vibrations as shown in Fig. 4(a). The pair of the bands at 3510 and 3573 cm^{-1} is located close to that of the bands at 3513 and 3595 cm^{-1} of species F, in which the O atom of the bidentate H_2O molecule accepts a single H-bond. The bands at 3397 and 3713 cm^{-1} are due to the singly H-bonded and free OH stretching vibrations of H_2O, respectively. Thus, in species H two H_2O molecules are H-bonded to B18C6 in the bidentate manner, and another H_2O molecule is singly H-bonded to either of the two bidentate H_2O molecules.

The IR-UV DR spectrum of species I [Fig. 4(b)] exhibits nine bands in the OH stretching region. Similar to the case of species H, the bands at 3202 and 3237 cm^{-1} are attributed to the bending overtone of H_2O components in species I. The 3308 and 3380 cm^{-1} bands are due to the singly H-bonded OH stretching vibrations. Apparently, two pairs of the bidentate OH vibrations appear in the 3450–3650 cm^{-1} region. The band at 3708 cm^{-1} is assigned to the free OH stretching vibration. The band pattern in the 3450–3750 cm^{-1} region is similar to that of species H [Fig. 4(a)]. The existence of the two singly H-bonded OH bands for species I suggests that one more H_2O molecule is attached to species H, resulting in a B18C6-$(H_2O)_4$ cluster of species I.

3.2.4 H-bond networks in B18C6-$(H_2O)_{1-4}$

Fig. 5 represents the hydration features of species A–I deduced from the IR-UV DR spectra. Species A–D have one bidentate H_2O molecule, which is referred to as w(B) in Fig. 5(a). For species E and G [Fig. 5(b)], there are two w(B) molecules. In species F [Fig. 5(c)], one H_2O molecule, w(B), is H-bonded to B18C6, and the other water molecule [w(D)] is H-bonded to the w(B). Species H [Fig. 5(d)] has a structure similar to that of species F, but with another w(B) molecule. In species I [Fig. 5(e)], an additional H_2O molecule is H-bonded to species H to form H-bonding chain; the middle H_2O molecule is referred to as w(AD). The sizes of species A–I were confirmed by mass-resolved two-color REMPI measurements as shown in ESI.

3.3 Conformation of B18C6

In order to determine the conformation of B18C6 theoretically, we carried out the geometry optimization and vibrational analysis of B18C6 at the B3LYP/6-31+G* level of theory. The geometry optimization resulted in 13 conformers in our calculations. Fig. 6 shows the 8 most stable conformers. The conformer I is the most stable one, and the relative energies of the conformers II–VIII are within 800 cm^{-1}. The other 5 conformers, which are not shown in Fig. 6, have the relative energies greater than 1150 cm^{-1}. Therefore, it is reasonable that species M1–M4 are attributed to the

conformers I–VIII. The conformation of species M1-M4 was investigated by comparing the observed IR spectrum in the CH stretching vibration region with the calculated ones. Fig. 7 shows the IR-UV DR spectra of species M1–M4 (a-d) and the calculated ones for I–VIII (e-l) in the CH stretching region. The solid curves in Fig. 7(e)–(l) are the calculated IR spectra produced by assuming the Lorentzian band shape with a full width at half maximum (FWHM) of 5 cm^{-1}. For ease of comparison, the IR-UV DR dip spectra are shown in an inverted manner. The IR bands in the 2800–3000 cm^{-1} region are attributed to the alkyl CH stretching vibrations of the crown ring. Although the IR spectral features of species M1–M4 are different from each other, some parts of the spectra of the M3 and M4 exhibit a very similar pattern as shown by dotted lines in Fig. 7(c) and (d). Therefore, species M3 and M4 are considered to have a similar conformation. The similarity of the conformation is consistent with the LIF result, which indicates that the bands M3 and M4 are located close to each other. However, since the agreement between the observed IR spectra and the calculated ones is not evident, it is not possible to determine the conformations of the M1–M4 by the comparison between the observed IR spectra and the calculated ones in the CH stretching region.

Other information that helps the structural assignment is the S_1–S_0 transition energy. In Fig. 8, the LIF spectra of B18C6 are compared with the electronic spectra calculated for conformers I–VIII (red bars). Here it is worth comparing the transition energy of B18C6 with that of 1, 2-dimethoxybenzene (DMB), which is the chromophore of B18C6 (Scheme 1). The calculated transition energies are scaled by the factor of 0.89599 so that the calculated transition energy of DMB (39901 cm^{-1}) fits to the observed value (35751 cm^{-1},[29] indicated by an arrow in Fig. 8). The bands M1–M4 of B18C6 are located on the lower-frequency side of the DMB origin band. In particular, the band M1 is located far from the DMB band. The electronic spectrum calculated for DMB monomer is shown in Fig. 8(k). Since the transition energy of the conformer IV is substantially higher than that of DMB, the conformer IV can be excluded from the candidates of species M1-M4. Among the other seven conformers (I–III and V–VIII), the conformer VIII shows the lowest transition energy, so we assign species M1 to the conformer VIII. In the geometry

optimization of B18C6-$(H_2O)_1$, the conformers II, V, and VII cannot accept a H_2O molecule with a stable bidentate H-bonding manner. As seen in the LIF spectra, the addition of water vapor reduces the intensities of the M2–M4 bands, suggesting that species M2–M4 can effectively incorporate H_2O molecule(s). Thus, the conformers II, V, and VII can be excluded from the candidates of M2–M4 species. As mentioned above, species M3 and M4 have a similar conformation. By comparing the structures of the conformers I, III, and VI (Fig. 6), one finds that the conformer I resembles the conformer VI. A small difference between the conformers I and VI is indicated by the circles in Fig. 6(a) and (f); the O atom in the circle points towards the center of the crown ring for the VI conformer, whereas out of the ring for the I conformer. On the other hand, the structures of the conformers I and VI are very different from that of the conformer III. Therefore, species M3 and M4 can be attributed to either of the conformers I and VI. As a result, species M2 can be ascribed to the conformer III, which has a substantially different conformation from those of the conformers I and VI. The band M2 is located on the lower-frequency side of the bands M3 and M4, in agreement with the calculated result, which suggests that the transition energy of the conformer III is lower than those of the conformers I and VI as seen in Fig. 8. Table 1 collects the positions of the origin band, cluster size, and structural assignment.

3.4 Structure of B18C6-$(H_2O)_1$

The structure of the hydrated clusters of B18C6 should be determined based on the analysis of the H-bonding structure and the conformation of B18C6. Useful information for the determination of the B18C6-$(H_2O)_n$ structure can be obtained by analyzing the CH and OH stretching vibrations, and the electronic transition energies. Fig. 9 displays the IR-UV DR spectra of B18C6-$(H_2O)_n$ (species B–I) in the CH stretching region. We could not observe the IR-UV DR spectrum of species A in the CH stretching region because of the weak intensity of band A. The IR spectra of species C–I show similar features to each other as highlighted by thick lines. This similarity strongly suggests that the hydrated clusters of species C–I have a similar conformation of the crown ring. On a

contrary, the IR spectrum of species B is different from those of species C–I, indicating that the crown-ring conformation for species B is quite different from those for species C-I .

In order to examine the relationship between the conformation of B18C6 and the encapsulation of water molecules, we performed the geometry optimization and vibrational analysis for B18C6-$(H_2O)_1$ at the B3LYP/6-31+G* level of theory. The geometry optimization of B18C6-$(H_2O)_1$ was started with the geometries of the conformers I–VIII (Fig. 6), to which one H_2O molecule is attached. We obtained more than 20 isomers of B18C6-$(H_2O)_1$. Among them, the 10 most stable isomers are shown in Fig. 10. The labeling of the isomers contains the information about the conformation of the B18C6 part and the number of H_2O molecules. For example, the isomer I-1W-1 [Fig. 10(a)] has the B18C6 conformation similar to that of the conformer I and encapsulates one H_2O molecule (1W). The digit at the end is used for identifying a specific isomer among the isomers having the same B18C6 conformation and the same number of H_2O molecules. Here, the isomer X-1W-1 [Fig. 10(c)] has another B18C6 conformation different from all those of the conformers I–VIII. The conformation of X is very similar to those of the conformers I and VI, that is, the difference among the conformers I, VI, and X lies in the small part of the crown ring indicated by the circles as shown in Fig. 10(a)–(c).

As mentioned above, the results of the LIF and IR-UV DR measurements for B18C6-$(H_2O)_1$ provide two structural conditions of B18C6-$(H_2O)_1$: (1) H_2O is H-bonded to the O atoms next to the benzene ring, and (2) H_2O is incorporated in the bidentate manner. Among the isomers shown in Fig. 10, the 6 most stable isomers [Fig. 10(a)–(f)] satisfy these conditions; the calculation well reproduces the structural preference deduced from the experiments. Therefore, the 6 most stable isomers can be the candidates for species A–D. It should be noted that in the 5 most stable isomers [Fig. 10(a)-(e)], one of the OH groups of H_2O is H-bonded to both O atoms (O_1 and O_{16}) adjacent to the benzene ring. This type of a H-bonding is called a "bifurcated" H-bond.[18,30]

The IR spectra calculated for the 6 most stable B18C6-$(H_2O)_1$ isomers in the OH stretching region are displayed in Fig. 2. It can be seen that all the calculated spectra well reproduce the IR-

UV DR spectra of species A–D. This means that one cannot simply assign each of species A–D to any of the 6 most stable isomers based on the OH stretching bands. So, we compared the observed electronic transition energies with the calculated ones. The calculated electronic transition energies for the six B18C6-$(H_2O)_1$ isomers are shown by the blue bars in Fig. 8. All the isomers show blue shifts with respect to the bare molecules. Since species A is located on higher-frequency side of the band M1 (VIII), species A can be attributed to the isomer VIII-1W-1. The similarity of the IR spectra in the CH stretching region (Fig. 9) suggests that species C and D have a similar B18C6 conformation to that of species E–I in larger clusters. Therefore, species C and D can incorporate additional H_2O molecules with no or small change in the B18C6 conformation. As we will explain in the next section, the conformer I cannot hold two bidentate H_2O molecules without changing its conformation. Since B18C6-$(H_2O)_1$ and B18C6-$(H_2O)_{2\text{-}4}$ have a similar B18C6 conformation as demonstrated by the IR spectra of the bands C-I, the isomers I-1W-1 and I-1W-2 are excluded from the candidates of species C and D. The difference between the conformers VI and X is quite small, and the isomers VI-1W-1 and X-1W-1 are considered to show similar IR spectra in the CH stretching region. Therefore, species C and D can be attributed to the isomers VI-1W-1 and X-1W-1, respectively. As for species B, we described that the conformation of the B18C6 part is quite different from those of species C, D and larger size clusters (E-I). The conformer III fits to this condition, since the conformation of the crown part in the isomer III-1W-1 [Fig. 10(d)] is completely different from that in the isomers VI and X. In addition, the conformer III does not form stable larger size B18C6-$(H_2O)_n$ ($n > 1$) clusters, which reproduce the observed IR spectra in the OH stretching region. Therefore, species B can be assigned to the isomer III-1W-1.

3.5 Structures of B18C6-$(H_2O)_{n>1}$

The similarity of the IR spectra for species C–I in the CH stretching region suggests that the B18C6 conformation in species E–I can be assigned to the conformer VI or X, because species C and D have the B18C6 conformation of the conformer VI or X. The IR spectra in the OH stretching

region indicate that species E–I have the hydration networks shown in Fig. 5(b)–(e). We carried out the geometry optimization and vibrational analysis for B18C6-$(H_2O)_{2–4}$. We utilized the initial geometries obtained by attaching H_2O molecules to the conformers I, VI, and X according to the features described in Fig. 5. Fig. 11 shows the optimized structures for B18C6-$(H_2O)_{2–4}$ formed on the conformer VI. The calculation for the conformation X also provides B18C6-$(H_2O)_{2–4}$ similar to those of the conformer VI in Fig. 11, although the clusters involving the conformer X are less stable than the corresponding ones of the conformer VI by a few hundreds cm^{-1}. As for the conformer I, it cannot incorporate two bidentate H_2O molecules different from VI-2W-1 and VI-2W-2 [Fig. 11(a) and (b)]. The failure in the formation of two bidentate H-bonds in the conformer I can be explained by the structural characteristics of VI-2W-1 and VI-2W-2. In these two clusters, the second H_2O molecules [referred to as w2 in Fig. 11(a) and (b)] are H-bonded to O_7 and O_{13} or to O_7 and O_1 in the bidentate manner. In the conformer I [Fig. 6(a)], on the other hand, O_7 atom is directed out of the crown ring. Therefore, it is difficult for the conformer I to accept a bidentate H_2O molecule using O_7. From these results, it is sufficient to consider the conformation of the crown part in B18C6-$(H_2O)_{2–4}$ as the conformer VI.

The IR spectra calculated for the isomers VI-2W-1, VI-2W-2, and VI-2W-3 are shown in Fig. 3. The IR spectrum of VI-2W-3 reproduces well the IR-UV DR spectrum of the band F. Thus, species F is attributed to the isomer VI-2W-3. The isomers VI-2W-1 and VI-2W-2 show different IR spectra, although both isomers have two bidentate H_2O molecules. In the case of the isomer VI-2W-1, two pairs of the bidentate OH stretching vibrations are close to each other, whereas those of the isomer VI-2W-2 are separated by ~30 cm^{-1}. These IR spectral features well reproduce the IR spectra of the bands E and G, respectively. Therefore, species E and G can be assigned to the isomers VI-2W-1 and VI-2W-2, respectively. The optimized structures of B18C6-$(H_2O)_{3,4}$ are shown in Fig. 11(d) and (e). The isomers VI-3W-1 and VI-4W-1 have the structures characteristic to those in Fig. 5(d) and 5(e) (???), and their IR spectra well reproduce the IR-UV DR spectra of the bands H and I as seen in Fig. 4. Thus, species H and I are assignable to the isomers VI-3W-1 and

VI-4W-1, respectively. The calculated S_1–S_0 transition energies of the isomers shown in Fig. 11 are displayed in Fig. 8(g) by the green bars. As the number of H_2O molecules increases, the transition energy is blue-shifted. This calculation tendency is consistent with the result of the LIF spectra. All the isomers of B18C6-$(H_2O)_{2\text{-}4}$ shown in Fig. 11 have one H_2O molecule (w1) H-bonded to the O atoms next to the benzene ring in the bidentate and bifurcated manners. Further hydration networks are extended on the isomer VI-1W-1; the first encapsulated water molecule plays a part in "nucleation" of the hydration.

Finally, we should mention the relative stability of the four species A-D of B18C6-$(H_2O)_1$. In the experiment, species D shows much stronger LIF intensity (Fig. 1) indicating an abundant population of species D. This suggests that the water encapsulation results in the formation of a specific conformer of B18C6. In the calculation we could not obtain such the specific conformer having large stabilization energy. Though it is not clear whether or not a higher level calculation gives such the specific isomer, the present study clearly demonstrates that water molecules change the conformation of B18C6 to better host the guest water molecules.

Conclusion

The relationship between the conformation and the hydration structure of B18C6 has been investigated by LIF, UV-UV hole-burning, REMPI, and IR-UV DR spectroscopy under the jet-cooled condition with the aid of quantum chemical calculations at the B3LYP/6-31+G* level of theory. The structural features are summarized as follows: (1) the number of B18C6 conformers is drastically reduced upon the hydration, and the H-bonding network of water molecules grows to both sides of the crown ring based on a specific conformer; (2) all the observed B18C6-$(H_2O)_n$ clusters have a common feature in which one H_2O molecule is H-bonded to the O atoms adjacent to the benzene ring in the "bidentate" and "bifurcated" manners.

Acknowledgment

This work is supported by Grant-in-Aid project (Grant Nos. 18205003 and 21350016) and MEXT for the Scientific Research on Priority Area "Molecular Science for Supra Functional Systems" (No. 477). YI would like to express his gratitude for the support of the Mitsubishi Chemical Corporation Fund.

References

1 G. Gokel, *Crown Ethers and Cryptands*, Royal Society of Chemistry: Cambridge, U. K., 1991.

2 M. Dobler, *Ionophores and their Structures*, Wiley-Interscience: New York, USA, 1981.

3 G. G. Talanova, N. S. A. Elkarim, R. E. Hanes, Jr., H. Hwang, R. D. Rogers, R. A. Bartsch, *Anal. Chem.* 1999, **71**, 672–677.

4 J. S. Benco, H. A. Nienaber, K. Dennen, W. G. McGimpsey, *J. Photochem. Photobiol. A* 2002, **152**, 33–40.

5 A. M. Stuart, J. A. Vidal, *J. Org. Chem.* 2007, **72**, 3735–3740.

6 A. N. Chekholov, *Russ. J. Coord. Chem.* 2008, **34**, 434–437.

7 D. Li, M. Du, J. Dou, D. Wang, *Z. Anorg. Allg. Chem.* 2005, **631**, 178-181.

8 T. Akutagawa, T. Motokizawa, K. Matsuura, S. Nishihara, S. Noro, T. Nakamura, *J. Phys. Chem. B* 2006, **110**, 5897–5904.

9 V. W. Bhagwat, H. Manohar, N. S. Poonia, *Inorg. Nucl. Chem. Lett.* 1981, **17**, 207–210.

10 N. S. Poonia, M. R. Truter, *J. Chem. Soc., Dalton Trans.* 1973, 2062–2065.

11 B. T. Gallagher, M. J. Taylor, S. R. Ernst, M. L. Hackert, N. S. Poonia, *Acta Cryst.* 1991, **B47**, 362–368.

12 R. D. Rogers, P. D. Richards, *J. Inclusion Phenom.* 1987, **5**, 631-638.

13 M. A. Belkin, A. V. Yarkov, *Spectrochim. Acta, Part A* 1996, **52**, 1475-1478.

14 C. Endicott, H. L. Strauss, *J. Phys. Chem. A* 2007, **111**, 1236-1244.

15 W. Wang, E. V. Ganin, M. S. Fonari, Y. A. Simonov, G. Becelli, *Org. Biomol. Chem.* 2005, **3**, 3054-3058.

16 D. Mootz, A. Albert, S. Schaefgen, D. Stäben, *J. Am. Chem. Soc.* 1994, **116**, 12045–12046.

17 K. Fukuhara, M. Tachikake, S. Matsumoto, H. Matsuura, *J. Phys. Chem.* 1995, **99**, 8617-8623.

18 M. Bühl, G. Wipff, *J. Am. Chem. Soc.* 2002, **124**, 4473–4480.

19 R. Kusaka, Y. Inokuchi, T. Ebata, *Phys. Chem. Chem. Phys.* 2007, **9**, 4452–4459.

20 R. Kusaka, Y. Inokuchi, T. Ebata, *Phys. Chem. Chem. Phys.* 2008, **10**, 6238–6244.

21 T. Ebata, T. Hashimoto, T. Ito, Y. Inokuchi, F. Altunsu, B. Brutschy, P. Tarakeshwar, *Phys. Chem. Chem. Phys.* 2006, **8**, 4783–4791.

22 Y. Inokuchi, Y. Kobayashi, T. Ito, T. Ebata, *J. Phys. Chem. A* 2007, **111**, 3209–3215.

23 M. J. Frisch, G. W. Trucks, H. B. Schlegel, G. E. Scuseria, M. A. Robb, J. R. Cheeseman, J. A. Montgomery, Jr., T. Vreven, K. N. Kudin, J. C. Burant, J. M. Millam, S. S. Iyengar, J. Tomasi, V. Barone, B. Mennucci, M. Cossi, G. Scalmani, N. Rega, G. A. Petersson, H. Nakatsuji, M. Hada, M. Ehara, K. Toyota, R. Fukuda, J. Hasegawa, M. Ishida, T. Nakajima, Y. Honda, O. Kitao, H. Nakai, M. Klene, X. Li, J. E. Knox, H. P. Hratchian, J. B. Cross, V. Bakken, C. Adamo, J. Jaramillo, R. Gomperts, R. E. Stratmann, O. Yazyev, A. J. Austin, R. Cammi, C. Pomelli, J. W. Ochterski, P. Y. Ayala, K. Morokuma, G. A. Voth, P. Salvador, J. J. Dannenberg, V. G. Zakrzewski, S. Dapprich, A. D. Daniels, M. C. Strain, O. Farkas, D. K. Malick, A. D. Rabuck, K. Raghavachari, J. B. Foresman, J. V. Ortiz, Q. Cui, A. G. Baboul, S. Clifford, J. Cioslowski, B. B. Stefanov, G. Liu, A. Liashenko, P. Piskorz, I. Komaromi, R. L. Martin, D. J. Fox, T. Keith, M. A. Al-Laham, C. Y. Peng, A. Nanayakkara, M. Challacombe, P. M. W. Gill, B. Johnson, W. Chen, M. W. Wong, C. Gonzalez, and J. A. Pople, *Gaussian 03*, Revision D.02,Gaussian, Inc., Wallingford CT, 2004.

24 G. Herzberg, *Molecular Spectra and Molecular Structure Volume II. Infrared and Raman Spectra of Polyatomic Molecules*, Krieger: Malabar, USA, 1991.

25 T. Watanabe, T. Ebata, S. Tanabe, N. Mikami, *J. Chem. Phys.* 1996, **105**, 408-419.

26 R. N. Pribble, T. S. Zwier, *Science* 1994, **265**, 75-79.

27 T. Ebata, K. Nagao, N. Mikami, *Chem. Phys.* 1998, **231**, 199–204.

28 Y. Nibu, R. Marui, H. Shimada, *J. Phys. Chem. A* 2006, **110**, 9627–9632.

29 J. T. Yi, J. W. Ribblett, D. W. Pratt, *J. Phys. Chem. A* 2005, **109**, 9456–9464.

30 N. Goutev, H. Matsuura, *J. Phys. Chem. A* 2001, **105**, 4741-4748.

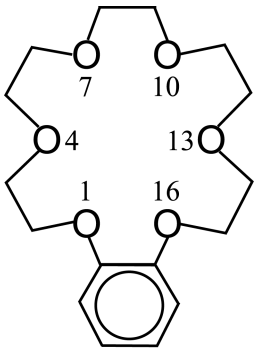

Scheme 1 B18C6

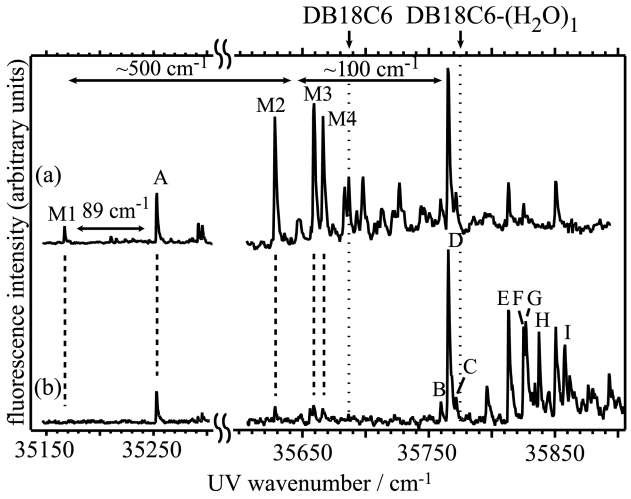

Fig. 1 LIF spectra of B18C6 and its hydrated clusters obtained (a) without and (b) with adding water vapor. Bands M1-M4 are due to bare B18C6 and bands A-I to B18C6-$(H_2O)_n$. The positions of the origin bands of DB18C6 and DB18C6-$(H_2O)_1$ are shown by arrows.

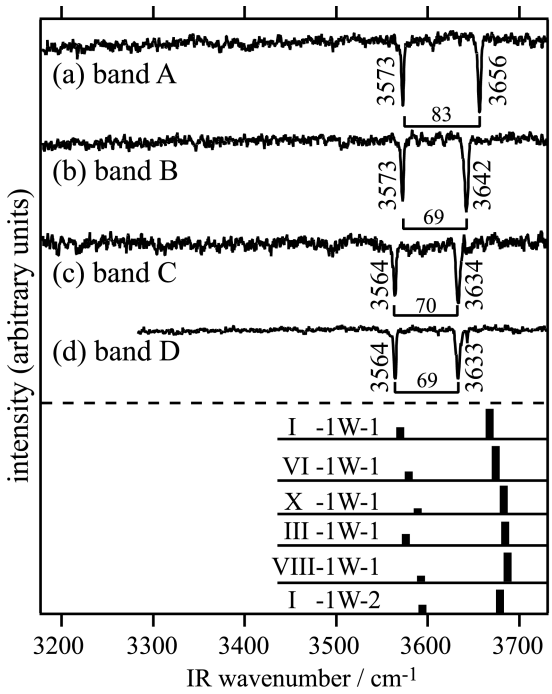

Fig. 2 IR-UV DR spectra obtained by monitoring bands A-D in the LIF spectra. The stick spectra represent IR spectra calculated for optimized structures of B18C6-$(H_2O)_1$.

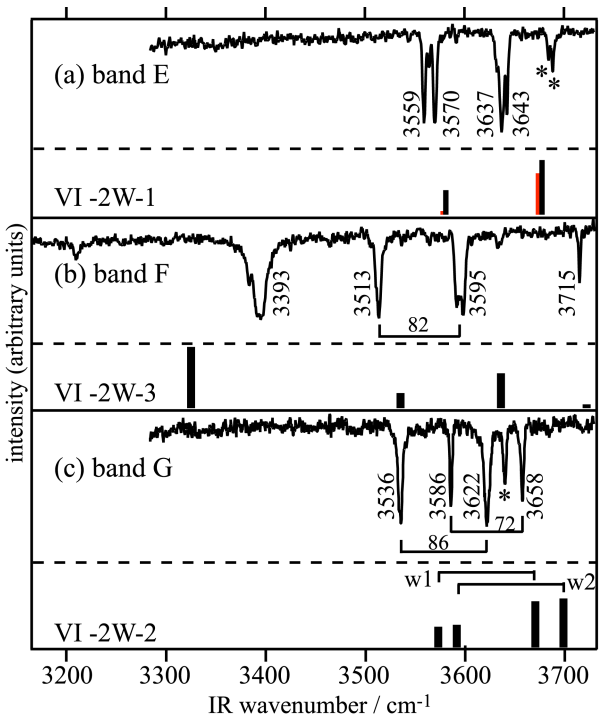

Fig. 3 IR-UV DR spectra obtained by monitoring bands E-G in the LIF spectra. The stick spectra represent IR spectra calculated for optimized structures of B18C6-$(H_2O)_2$. In the calculated spectrum of VI-2W-1, two pairs of the bidentate OH stretching vibrations (red and black sticks) are located close to each other.

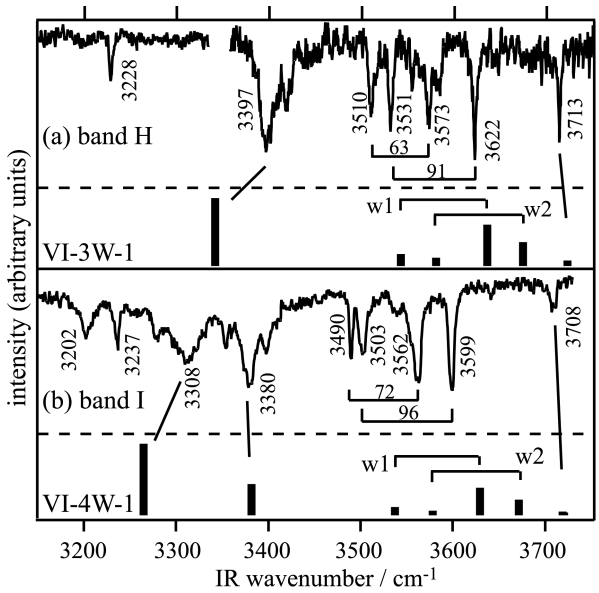

Fig. 4 IR-UV DR spectra obtained by monitoring bands H and I in the LIF spectra. The stick spectra represent IR spectra calculated for optimized structures of B18C6-$(H_2O)_{3,4}$.

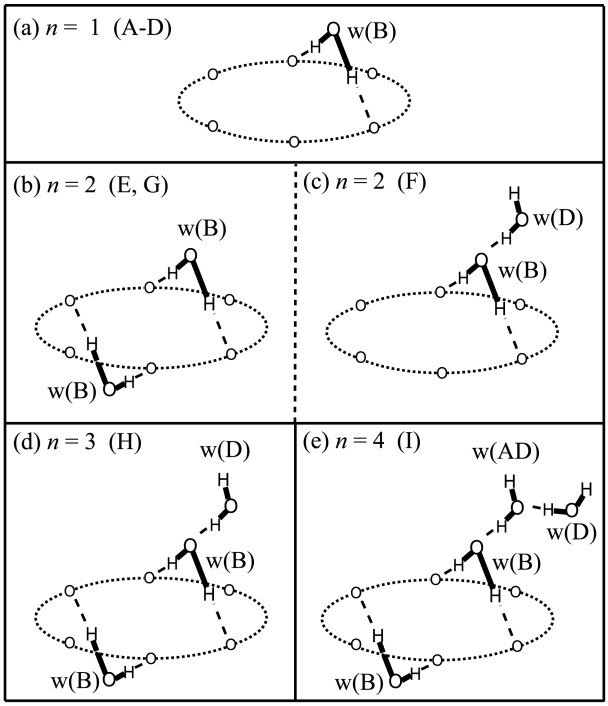

Fig. 5 Geometric features deduced from the IR-UV DR results of species A-I. In this figure, w(B) and w(D) stand for the bidentate and singly H-bonded H_2O molecules, respectively. The H_2O molecule labeled as w(AD) takes part in H-bonding acceptance and donation.

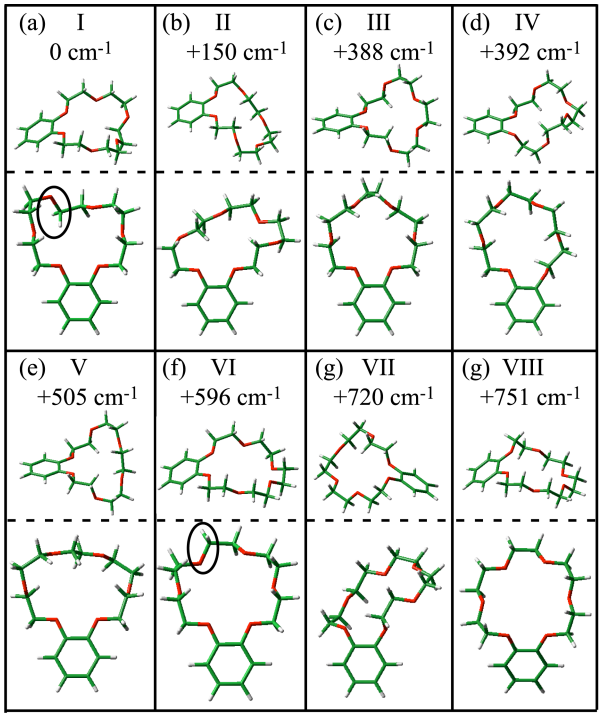

Fig. 6 Optimized structures of bare B18C6 at the B3LYP/6-31+G* level. Top and side views are shown for each isomer. The numbers shown in cm^{-1} unit represent the total energy of the conformers relative to that of the most stable one (conformer I). Conformers I and VI are similar to each other; only the orientation of the O atoms highlighted by the solid circles in Fig. 6(a) and 6(f) is different.

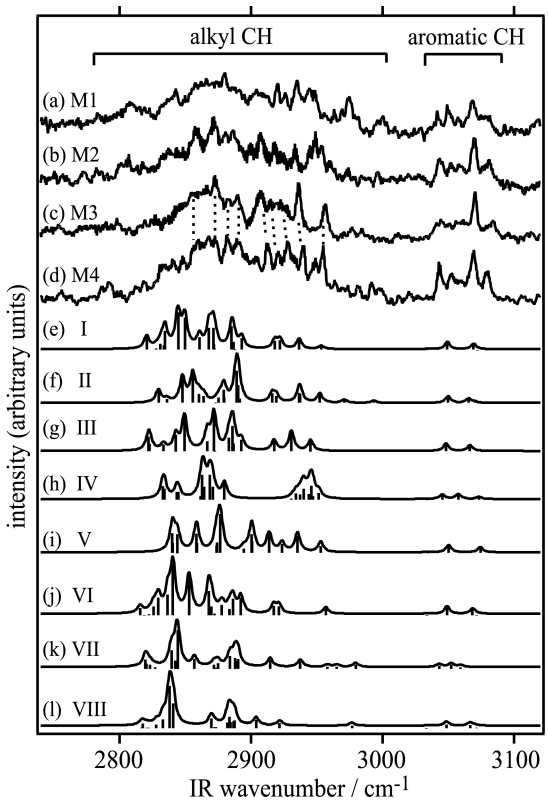

Fig. 7 (a-d) IR-UV DR spectra of species M1-M4 in the CH stretching region. (e-l) IR spectra calculated for conformers I-VIII in Figure 6 at the B3LYP/6-31+G* level. The solid curves are IR spectra reproduced by providing Lorentzian components with a FWHM of 5 cm^{-1} for all the calculated IR bands.

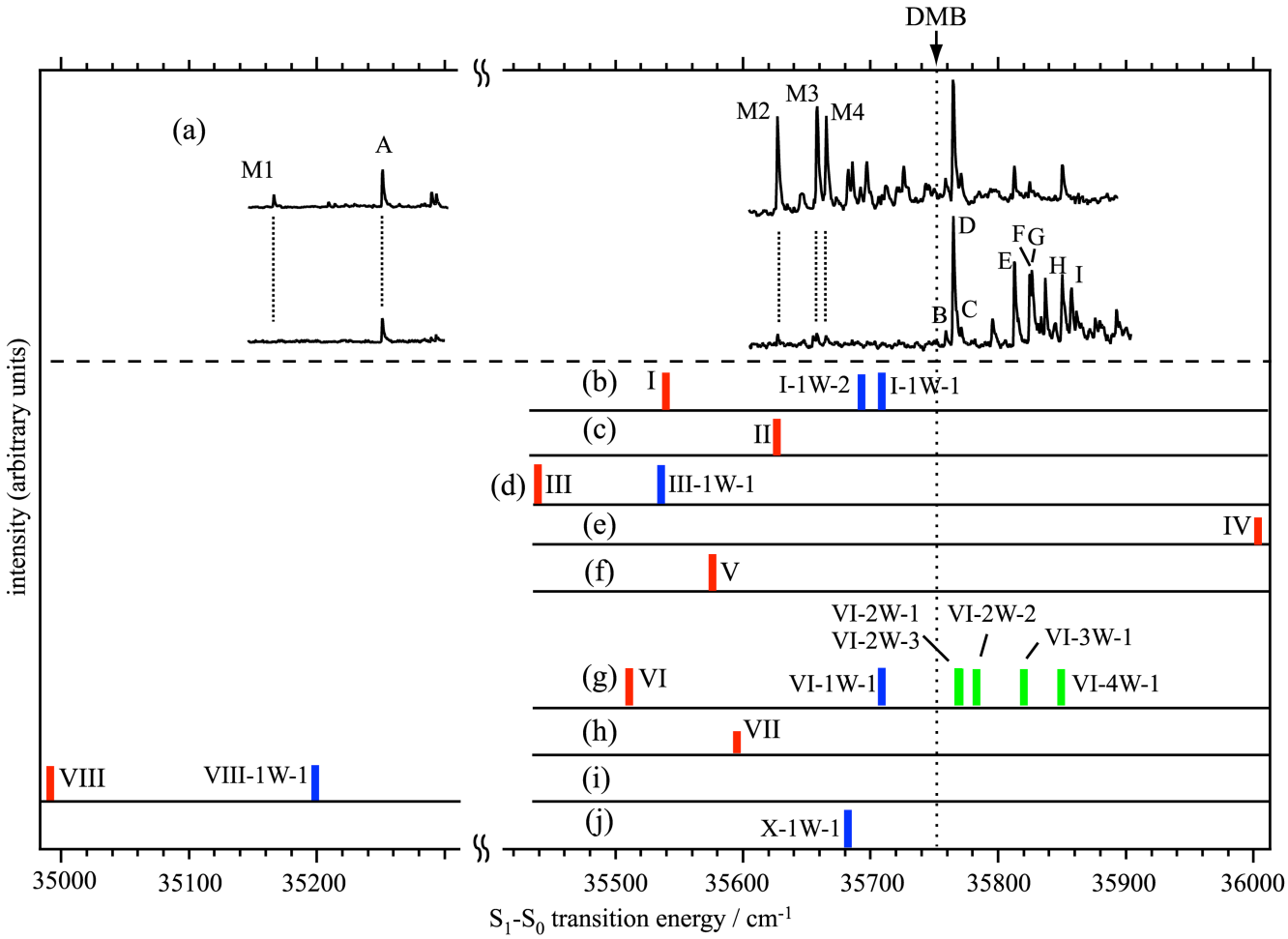

Fig. 8 (a) LIF spectra of B18C6. (b-j) S_1-S_0 electronic spectra calculated for B18C6-$(H_2O)_{0-4}$ isomers with TDDFT method at the B3LYP/6-31+G* level. The red, blue, and green bars represent the electronic transition of bare B18C6, B18C6-$(H_2O)_1$, and B18C6-$(H_2O)_{2-4}$, respectively. The results of the isomers that have the same conformation in the B18C6 part are drawn in the same row. The height of the bars shows the oscillator strength of the electronic transition. The calculated spectra are scaled by 0.89599 as the calculated transition energy of DMB (39901 cm^{-1}) corresponds to observed one (35751 cm^{-1}). The position of the origin band of DMB (35751 cm^{-1}) is shown by an arrow.

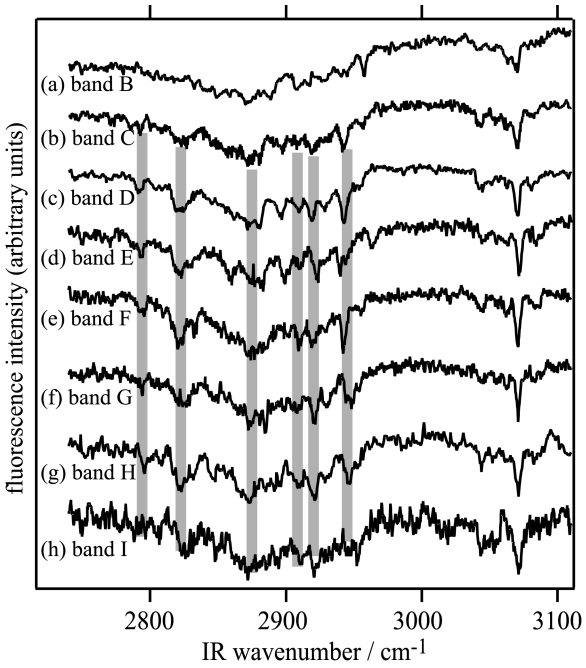

Fig. 9 IR-UV DR spectra of bands B-I in the CH stretching region. Thick lines highlight similar features in the spectra of bands C-I at ~2790, ~2820, ~2870, ~2910, ~2920, and ~2940 cm^{-1}.

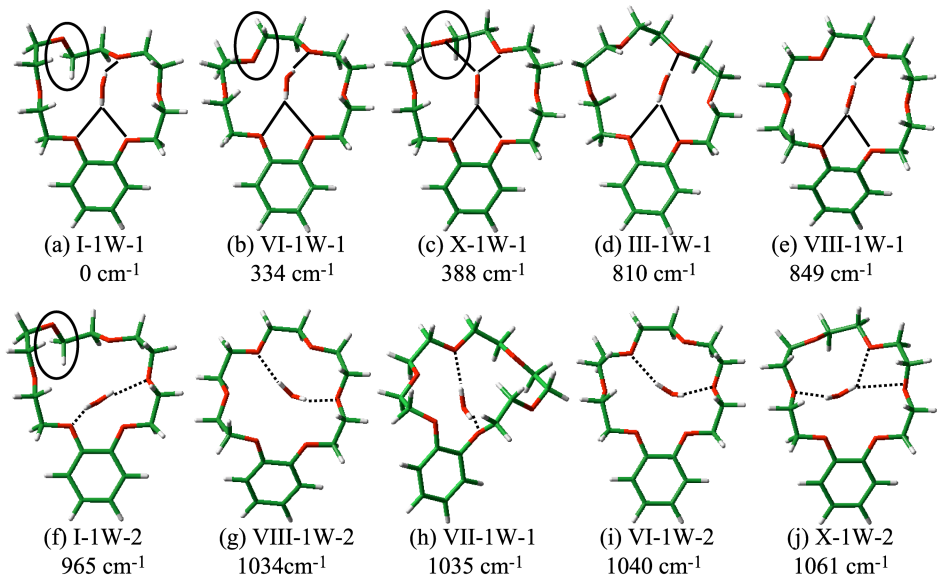

Fig. 10 Optimized structures of B18C6-$(H_2O)_1$ at the B3LYP/6-31+G* level.
The numbers shown in cm^{-1} unit represent the total energy of the isomers relative to that of the most stable one (isomer I-1W-1). The solid and dotted lines in the H-bonding are used to express the side of B18C6 on which water molecules form H-bonding.

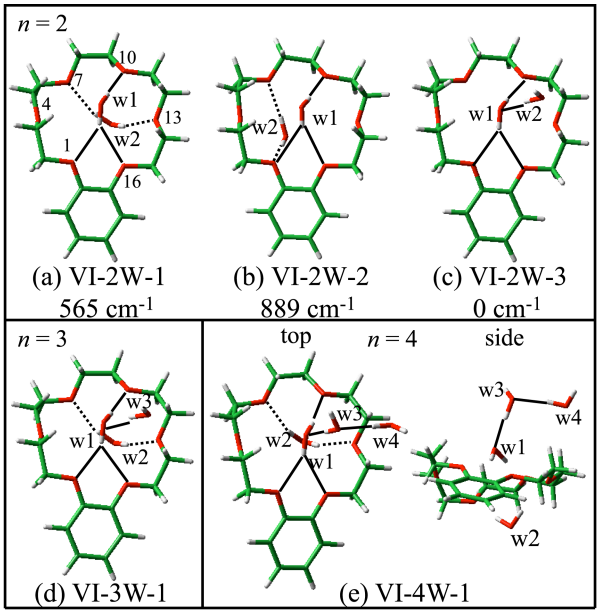

Fig. 11 Optimized structures of (a-c) B18C6-$(H_2O)_2$ and (d, e) B18C6-$(H_2O)_{3,4}$ at the B3LYP/6-31+G* level. The numbers shown in cm^{-1} unit represent the total energy of the isomers relative to that of VI-2W-3. The solid and dotted lines in the H-bonding are used to express the side of B18C6 on which water molecules form H-bonding.

Table 1 The positions of the S_1-S_0 origin band, cluster size, and structural assignment for species M1-M4 and A-I.

Species	Position / cm^{-1}	Cluster Size	Assignment
M1	35167	B18C6	VIII
M2	35628		III
M3	35659		I or VI
M4	35666		I or VI
A	35253	B18C6-$(H_2O)_1$	VIII-1W-1
B	35758		III-1W-1
C	35771		VI-1W-1 or X-1W-1
D	35766		VI-1W-1 or X-1W-1
E	35813	B18C6-$(H_2O)_2$	VI-2W-1
F	35825		VI-2W-3
G	35827		VI-2W-2
H	35837	B18C6-$(H_2O)_3$	VI-3W-1
I	35858	B18C6-$(H_2O)_4$	VI-4W-1

A graphical and textual abstract

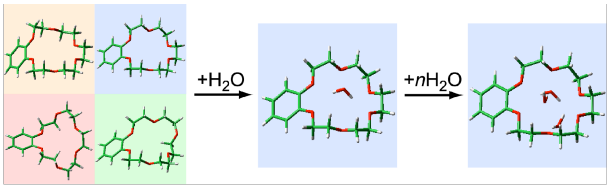

Water molecules are encapsulated preferentially by a specific conformer of benzo-18-crown-6-ether, and they develop hydrogen bonding networks in its cavity.